A&A 482, 535–539 (2008)
DOI: 10.1051/0004-6361:20079259

Astronomy & Astrophysics

Detection of 6 K gas in Ophiuchus D

J. Harju[1], M. Juvela[1], S. Schlemmer[2], L. K. Haikala[1], K. Lehtinen[1], and K. Mattila[1,⋆]

[1] Observatory, PO Box 14, 00014 University of Helsinki, Finland
e-mail: jorma.harju@helsinki.fi
[2] I. Physikalisches Institut, Universität zu Köln, Zülpicher Straße 77, 50937 Köln, Germany

Received 17 December 2007 / Accepted 18 January 2008

ABSTRACT

Context. Cold cores in interstellar molecular clouds represent the very first phase in star formation. The physical conditions of these objects are studied in order to understand how molecular clouds evolve and how stellar masses are determined.
Aims. The purpose of this study is to probe conditions in the dense, starless clump Ophichus D (Oph D).
Methods. The ground-state ($1_{10} \rightarrow 1_{11}$) rotational transition of *ortho*-H_2D^+ was observed with APEX towards the density peak of Oph D.
Results. The width of the H_2D^+ line indicates that the kinetic temperature in the core is about 6 K. So far, this is the most direct evidence of such cold gas in molecular clouds. The observed H_2D^+ spectrum can be reproduced with a hydrostatic model with the temperature increasing from about 6 K in the centre to almost 10 K at the surface. The model is unstable against any increase in the external pressure, and the core is likely to form a low-mass star.
Conclusions. The results suggest that an equilibrium configuration is a feasible intermediate stage of star formation even if the larger scale structure of the cloud is thought to be determined by turbulent fragmentation. In comparison with the isothermal case, the inward decrease in the temperature makes smaller, i.e. less massive, cores susceptible to externally triggered collapse.

Key words. ISM: clouds – ISM: molecules – ISM: kinematics and dynamics – ISM: individual objects: ρ Oph, core D (L1696A) – stars: formation

1. Introduction

Starless cores of molecular clouds are heated externally by the interstellar radiation field (ISRF) and by cosmic rays. Theoretical estimates of the attenuation of the ISRF by dust suggest that the temperature decreases to about 5–6 K in the centres of dense starless cores (Evans et al. 2001; Zucconi et al. 2001; Stamatellos & Whitworth 2003). Observational evidence of low temperatures is still scarce.

Direct measurement of the gas properties, such as the kinetic temperature, is possible using spectral lines. Spectral line observations of very dense, starless cores are, however, hampered by the fact that common tracer molecules like CO and CS freeze there onto dust grains (Willacy et al. 1998; Caselli et al. 1999). The nitrogenous compounds NH_3 and N_2H^+ seem to survive longer than most other species (Tafalla et al. 2006). This is fortunate because the rotational temperature of NH_3 is considered to be a good measure of the kinetic temperature. Recently NH_3 excitation was used to derive a very low gas temperature, ~5.5 K, in the centre of the prestellar core L1544 in Taurus (Crapsi et al. 2007).

At very high densities ($n \sim 10^6$–10^7 cm^{-3}) and low temperatures ($T < 10$ K) also NH_3 and N_2H^+ are likely to freeze out, and the gallery of useful molecular tracers becomes very limited (Walmsley et al. 2004). In these circumstances the abundances of H_3^+, and its energetically favoured deuterated forms, H_2D^+, D_2H^+, and D_3^+, are predicted to increase strongly. The asymmetric isotopologues H_2D^+ and D_2H^+ have permanent electric dipole moments, so can be used as probes of these otherwise hidden regions (Caselli et al. 2003; Vastel et al. 2004; van der Tak et al. 2005).

Here we use the singly deuterated trihydrogen ion, H_2D^+, to show that the gas kinetic temperature is about 6 K in the very dense core of the starless clump Oph D (L1696A), which lies in the nearby ρ Ophiuchii molecular cloud. The position observed is located near the southern tip of the elongated clump. It corresponds to the thermal dust emission maximum at $\lambda = 850\,\mu$m on the SCUBA map of Kirk et al. (2005), and the dust *absorption* maximum on the ISOCAM 7 μm map of Bacmann et al. (2000). This position coincides with the N_2D^+ peak in the survey of Crapsi et al. (2005; see their Fig. 10), and represents the density and column density maximum of the clump. The 3D structure of the whole clump has been recently modelled by Steinacker et al. (2005).

2. Observations and data reduction

The observations were made with APEX on May 15, 2006. The telescope is described by Güsten et al. (2006). The 372 421.364 MHz line of *ortho*-H_2D^+ was observed in the upper sideband of the APEX-2A SIS DSB receiver. The HPBW of the antenna is 17″ at this frequency. The backend was the Max-Planck-Institut für Radioastronomie Fourier transform spectrometer (FFTS). The 1 GHz band of the FFTS was divided into 16 384 channels resulting in a channel width of 61 kHz which corresponds to ~50 m s^{-1} at the observed frequency. The effective resolution of the spectrometer corresponds to 80 m s^{-1}. The observations were performed in the position-switching

⋆ This publication is based on data acquired with the Atacama Pathfinder Experiment (APEX). APEX is a collaboration between the Max-Planck-Institut für Radioastronomie, the European Southern Observatory, and the Onsala Space Observatory.

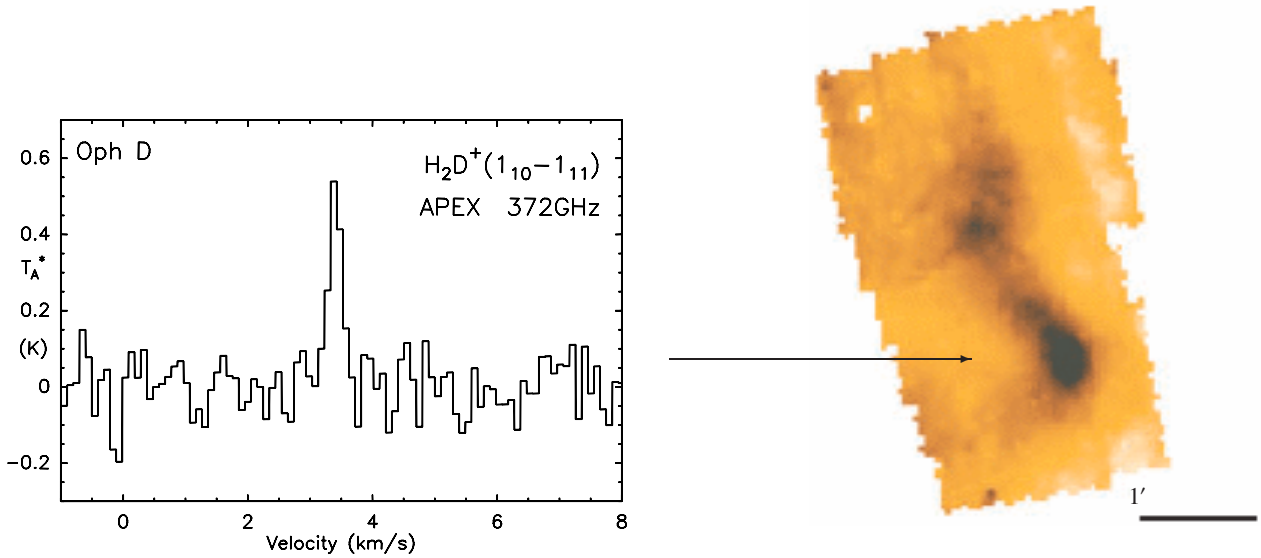

Fig. 1. *Left*: the H_2D^+ spectrum towards Oph D. *Right:* ISOCAM 7 μm mid-infrared absorption image of the Oph D clump obtained by Bacmann et al. (2000; the image is reproduced from Bergin & Tafalla 2007). The scale is indicated by a 1′ bar.

mode. The coordinates of the ON-position are RA $16^h28^m28\overset{s}{.}9$, Dec $-24°19'09''$ (J2000). The OFF-position was selected $-10'$ south of ON-position in Dec. The spectrum shown in Fig. 1 has been obtained by adding 60 ON-OFF measurements with a duration of 20 s per phase. The observed position is indicated on the 7 μm ISOCAM absorption map of Bacmann et al. (2000; reproduced from Bergin & Tafalla 2007). The observing conditions were good (PVW 0.34 mm, zenith opacity 0.33 at 372 GHz). Oph D was in the elevation range 60°–70°, and the DSB system temperature was about 210 K during these measurements.

The observed spectra were reduced in a standard way using the GILDAS software package[1]. The occasional low-frequency ripple in the individual raw spectra was first fit with a sinusoidal baseline, after which possible higher frequency ripple was masked out in Fourier space. After averaging the 60 individual spectra, a first-order baseline was subtracted.

3. Results

The detected H_2D^+ line has a single, narrow component. A Gaussian fit to the spectrum gives the following line parameters: $T_A^* = 0.60 \pm 0.09$ K, $v_{LSR} = 3.40 \pm 0.01$ km s^{-1}, and Δv(FWHM) $= 0.26 \pm 0.03$ km s^{-1}. The molecular mass of H_2D^+ is only 4 a.m.u. The observed linewidth, if assumed to be caused only by thermal broadening, indicates a kinetic temperature of $T_{kin} = 6.0 \pm 1.4$ K. This is an upper limit as the estimate neglects the possible non-thermal broadening and the slight instrumental broadening, the contribution of which is about 0.01 km s^{-1}.

4. Discussion

The temperature obtained towards Oph D is similar to the estimate for the nucleus of L1544 mentioned above (Crapsi et al. 2007). The present determination is more direct than that in L1544 because it does not involve modelling. These two results using very different methods consolidate evidence of very low temperatures inside starless dense cores.

[1] Grenoble Image and Line Data Analysis Software package has been developed by IRAM-Grenoble, see
http://www.iram.fr/IRAMFR/GILDAS

The H_2D^+ position coincides with the N_2D^+ maximum of the core with an exceptionally high N_2D^+/N_2H^+ column density ratio (Crapsi et al. 2005). The enhancement of N_2D^+ is caused by the precursor molecule N_2 reacting with increasingly abundant H_2D^+, D_2H^+ or D_3^+ instead of the normal isotopologue H_3^+. Carbon monoxide has been observed to be heavily depleted in this core (Bacmann et al. 2002). The accumulated observational results, i.e. CO depletion, a large degree of deuterium fractionation, the detection of H_2D^+, and a very low kinetic temperature, all fit qualitatively into the current picture of chemistry in dense starless cores (Walmsley et al. 2004).

The picture is not complete, however, until we manage to build a physical model for the object to explain the observed H_2D^+ profile. The dense central core observed here apparently has very little turbulence and looks roundish in the N_2D^+ maps (Crapsi et al. 2005). It may therefore be in near hydrostatic equilibrium. As the H_2D^+ line, which probably originates in the core centre, indicates a very low temperature, it is reasonable to assume a radial temperature gradient. We adopt the modified Bonnor-Ebert model (Evans et al. 2001; Zucconi et al. 2001), i.e., a self-gravitating, hydrostatic core with a temperature gradient caused by the attenuation of the ISRF. As the condensation is part of a larger cloud, we assume, somewhat arbitrarily, that the obscuration by the surrounding envelope corresponds to a visual extinction of $A_V = 10^m$. This choice is of little importance because the obscuration by the core itself must be much higher to produce a temperature close to 6 K in the centre.

4.1. Core model

The density and temperature distributions in the core were solved in an iterative manner. The density distribution was first solved for an isothermal Bonnor-Ebert sphere (Alves et al. 2002), and the radial temperature gradient was calculated using the ISRF and dust opacity models adopted from the literature (Black 1994; Ossenkopf & Henning 1994). This temperature distribution was used to derive a new density profile by integrating the equation of hydrostatic equilibrium.

We assumed that the gas temperature, T_{kin}, is equal to the dust temperature, T_{dust}. This assumption is generally believed to be valid at densities relevant to this study (>10^5 cm^{-3},

Burke & Hollenbach 1983). Recently, Bergin et al. (2006) found evidence of different gas and dust temperatures in the centre of the globule B68 with $n(H_2) \sim 3 \times 10^5$ cm^{-3}. We note, however, that the nearly 10 times higher density in Oph D is likely to result in a closer dust-gas thermal coupling as compared with B68.

All radiative transfer calculations were made using our Monte Carlo code (Juvela 1997). It was found that central densities in excess of 10^6 cm^{-3} are needed to make the temperature decrease close to 6 K. As a test, we compared the temperature profile calculation with the results of Stamatellos & Whitworth (2003). Identical temperature distributions were obtained using the same models for the core stucture, ISRF spectrum, and the dust opacity.

4.2. H_2D^+ excitation

The structure and rotational spectrum of H_2D^+ are well known (Miller et al. 1989). Like molecular hydrogen, H_2, the molecule has two nuclear spin states, *ortho* (hereafter o-H_2D^+, the H nuclei have parallel spins), and *para* (p-H_2D^+, opposite spins). While radiative transitions are only possible between rotational levels of the same nuclear spin state, collisions with H_2 can also result in ortho-para conversion (e.g., Gerlich et al. 2002).

The state-to-state coefficients for the $H_2D^+ + H_2$ system are not available. In the recent study of H_2D^+ profiles towards L1544 van der Tak et al. (2005) used scaled radiative rates adopted from Black et al. (1990), where the downward collisional coefficients within the ortho and para ladders were assumed to be proportional to the line strengths of the corresponding radiative transitions, and a constant value was used for downward inter-ladder transitions. The upward rates were evaluated by using the principle of detailed balancing.

A microcanonical statistical study of the reaction $H_3^+ + H_2$ has been published recently (Park & Light 2007). This treatment is being applied to the deuterated isotopologues, but the state-to-state reaction probabilities for $H_2D^+ + H_2$ have not yet been calculated (Hugo et al. 2007). In the present paper the collisional coefficients were calculated using a modification of the Oka & Epp (2004) model. The coefficients are normalized to conform with the available chemical data on the nuclear spin-changing reactions. The assumptions and parameter values used in the calculation are available in the Appendix. The approximation corresponds to the canonical approach discussed in Hugo et al. (2007).

The core model and the collisional coefficients were used to calculate the populations of the rotational levels of H_2D^+, and $H_2D^+(1_{10} \rightarrow 1_{11})$ line profiles towards the core centre. The calculated spectrum corresponds to the source brightness temperature distribution convolved with the 17″ APEX beam. The central density and the outer radius of the core and the total (o+p) H_2D^+ abundance were varied, and the resulting line profile was compared with the observed one. Our best-fit H_2D^+ spectrum and the corresponding core model are shown in Fig. 2. The model spectrum was converted to the T_A^* scale by multiplying it by the main-beam efficiency, $\eta_{MB} = 0.73$.

4.3. Modelling results

The line *intensity* can be reproduced by a set of hydrostatic models with the central density and the central temperature ranging from 2×10^6 cm^{-3} to 1×10^7 cm^{-3}, and from 6.8 K to 6.1 K, respectively. The best-fit model has a central density of 4×10^6 cm^{-3}. In this model the temperature decreases from

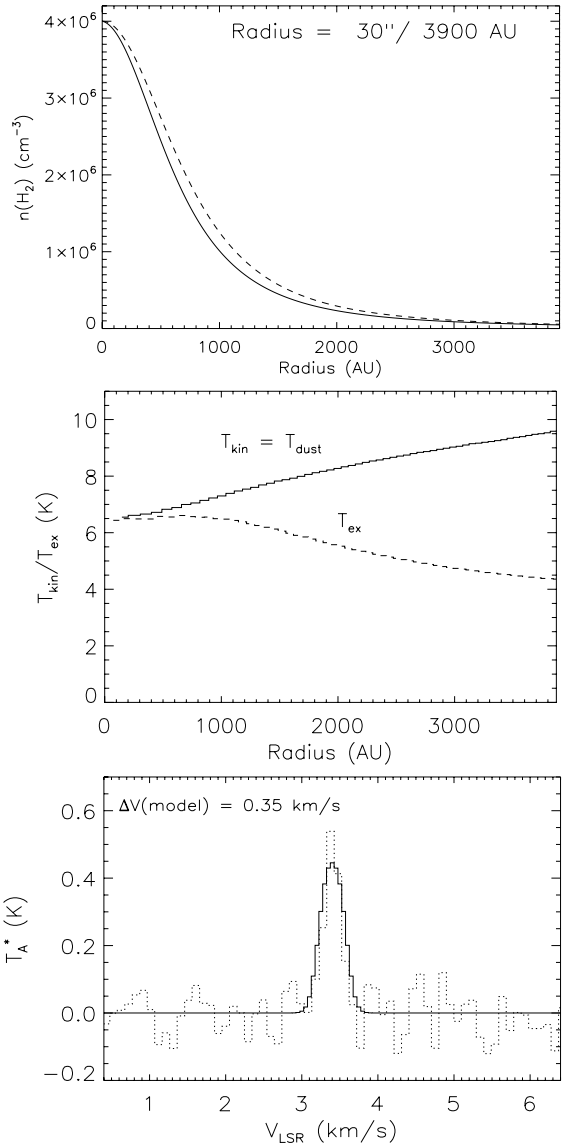

Fig. 2. The core model and the calculated H_2D^+ spectrum. *Top*: density as a function of radial distance from the core centre according to our hydrostatic, non-isothermal model (continuous line). For comparison the solution for an isothermal sphere with $T_{kin,iso} = \langle T_{kin} \rangle = 8.3$ K and the same peak density is shown as a dashed line. *Middle*: The radial profiles of the kinetic temperature, T_{kin} (assumed to be equal to T_{dust}), and the excitation temperature of the line, T_{ex}. The line is thermalized in the core centre, but becomes subthermally excited towards the edge as the density decreases. *Bottom:* $H_2D^+(1_{10} \rightarrow 1_{11})$ spectrum (in the T_A^* scale) resulting from the Monte Carlo radiative transfer calculations applied to the hydrostatic model presented in *the two upper panels*. The observed spectrum is shown as a dotted line.

9.6 K at the surface to 6.4 K in the centre. The line *width* of the corresponding model spectrum is 0.35 km s^{-1}. This and all model spectra having similar peak intensity are broader than the observed one. There are two reasons for this: 1) the kinetic temperature in the centre of the model is slightly higher than 6 K, and 2) the peak optical thickness of the line must be close to unity to give sufficiently high intensity. Opacity broadening is responsible for about one half of the "extra" linewidth (~0.1 km s^{-1}) of the best fit spectrum with $\tau_{peak} \sim 1.1$. This τ value results from a total H_2 column density of 1×10^{23} cm^{-2} and a fractional H_2D^+ abundance of 5×10^{-10}. The core mass is nearly the same, 0.25 $M_\odot$, for all hydrostatic models quoted

above. The outer radius was assumed to be 3900 AU (apparent radius 30″). This is consistent with the published maps (Kirk et al. 2005; Crapsi et al. 2005). We assume a distance of 130 pc (Knude & Høg 1998).

The core can be made cooler by increasing the central density further. This would, however, decrease the line intensity because of a larger optical thickness and beam-dilution effects as the brightness distribution becomes more centrally peaked.

We also calculated temperature distributions and H_2D^+ spectra for the density profiles derived previously for Oph D by Motte et al. (1998) and Bacmann et al. (2000), who used millimetre dust continuum emission and mid-infrared absorption, respectively. These models assume a constant density within a radius of 20″–25″ from the core centre, and a power law in the outer envelope up to 85″. For the Motte et al. (1998) model, with a central density of 9×10^5 cm^{-3}, the calculated temperature goes down to 6.1 K in the centre. The Bacmann et al. (2000) model with a lower central density (3×10^5 cm^{-3}) gives a minimum temperature of 7.4 K. The model of Motte et al. produces similar H_2D^+ spectra to the hydrostatic models quoted above. The existence of a large, homogenous, and non-turbulent nucleus could possibly be justified by invoking a stabilizing magnetic field.

In view of the moderate S/N of the observed H_2D^+ line and the uncertainties related to the collisional coefficients, the hydrostatic model gives a reasonably good fit to the observed spectrum. A high S/N H_2D^+ spectrum towards this source, together with rigorously derived collisional coefficients will show if the slightly "too bright and too narrow" line remains a problem. Assuming that the excitation within the ortho and para ladders is thermal, the H_2D^+ spectrum constrains the model parameters in the following way. 1) In order to reproduce both the observed intensity and linewidth, the central temperature must be about 6 K but not much less. The minimum temperature sets a limit to the maximum density through the adopted ISRF and dust opacity models. 2) The H_2D^+ line is preferably optically thin, and in any case the peak optical thickness cannot be much larger than unity. For high opacities, the line peak flattens and the FWHM becomes clearly larger than observed. This determines the upper limit of the column density and the fractional abundance of the molecule. According to the adopted model for ortho-para transitions, the o/p ratio of H_2D^+ increases as the temperature decreases, and consequently, in the centre most H_2D^+ is in ortho states. This effect facilitates the detection of H_2D^+ in cold cores. Furthermore, the accuracy of the modelling results is improved by nearly all H_2D^+ molecules being in the two states coupled by the observed transition.

According to Steinacker et al. (2005) the elongated structure of the Oph D clump is likely to have formed as a result of turbulent fragmentation. They suggest that the southern condensation (i.e. the core observed here) may be gravitationally bound and collapsing. The present observation and modelling conform with the idea of a self-gravitating core, but the very narrow line profile suggests that the collapse has temporarily halted.

Compared with an isothermal core at a kinetic temperature $T_{\rm kin,iso}$, a core with inward decreasing temperature with the same central density and the average temperature $\langle T_{\rm kin}\rangle = T_{\rm kin,iso}$ has a smaller critical radius (Alves et al. 2002) beyond which the core becomes unstable against an increase of the external pressure. While for an isothermal sphere the critical dimensionless radius parameter, ξ, is 6.45, the corresponding parameter for our best-fit model is 6.20. This value corresponds to 1700 AU (13″), which is clearly smaller than the core radius derived in previous studies. Even though the effect might be marginal, we note that the temperature gradient signifies that smaller and less massive cores are susceptible to externally triggered collapse.

5. Conclusions

The modelling results presented above depend on several unknown factors, above all the collisional coefficients of H_2D^+ and the possible local variations in the ISRF and the dust properties. Nevertheless, the observed H_2D^+ spectrum can be reproduced reasonably well by a self-consistent physical model. The strength of H_2D^+ is that it selectively traces the dense nuclei of cold cores, and can therefore be used to study their internal structure.

In Oph D we seem to be witnessing a quiescent phase of core evolution. The modelling results suggest, however, that the balance can be easily disturbed and that the core will eventually collapse. The possibility of a temporary equilibrium configuration is interesting as it has been suggested that Oph D was formed by turbulent fragmentation (Steinacker et al. 2005).

The usefulness of H_2D^+ in studies of the early stages of star formation has been predicted by astrochemists and modellers (e.g. Bergin et al. 2002). Emerging high-altitude radio telescopes, most recently APEX, are providing empirical tests of these ideas.

Acknowledgements. We thank the APEX staff, especially Andreas Lundgren and Felipe Mac-Auliffe, who performed the observations, and Per Bergman, who carefully checked that the intensity calibration is correct. The Helsinki group acknowledges support from the Academy of Finland through grants 117206, 1210518, 115056, and 107701.

Appendix A: Approximation for the collisional rates of H_2D^+

In the calculation of the state-to-state rate coefficients, we have adopted the approximation used by Oka & Epp (2004) for H_3^+ + H_2 collisions. This approximation is based on the principles of complete randomness and a detailed balance of upward and downward transitions between any two levels. This model does not consider any nuclear spin restrictions. It is known, however, that in cold gas the conversion between the para and ortho states of H_2D^+ occurs predominantly via collisions with o-H_2. The following reactive transitions are possible (Gerlich et al. 2002; Walmsley et al. 2004):

$$\mathrm{p-H_2D^+ + o-H_2} \underset{k_1^-}{\overset{k_1^+}{\rightleftharpoons}} \mathrm{o-H_2D^+ + p-H_2} \quad \text{(A.1)}$$

$$\mathrm{o-H_2D^+ + o-H_2} \underset{k_2^-}{\overset{k_2+}{\rightleftharpoons}} \mathrm{p-H_2D^+ + p-H_2}. \quad \text{(A.2)}$$

In molecular clouds the *ortho/para* ratio of H_2, o/p-H_2, is likely to be non-thermal (i.e., more o-H_2 than expected from thermodynamic equilibrium where o/p-$H_2 \sim 9e^{-170.4{\rm K}/T}$) (Gerlich et al. 2002; Walmsley et al. 2004; Flower et al. 2006). Consequently, reaction (A.1) pumps H_2D^+ from para to ortho states with the help of the internal energy of o-H_2, and this effect becomes more marked at low temperatures where the endothermic "backward" reaction is inhibited.

Because of the small fraction of o-H_2, the total rates of the nuclear spin changing reactions are likely to be much lower than those derived from the Oka & Epp approximation. We have therefore scaled the Oka & Epp coefficients to be consistent with the total rates of the nuclear spin-changing reactions (A.1)

and (A.2). The assumptions used in the calculation are summarised below.

1) The total rate coefficient of rotationally inelastic and nuclear spin reactive $H_2D^+ + H_2$ collisions, k_C, corresponds to that given by the Oka & Epp (2004) approximation at the same temperature. The total number of collisions per cm^3 and s is $k_C n(H_2) n(H_2D^+)$. The coefficient k_C can be expanded in terms of state-to-state coefficients, $C_{i,f}$, as

$$k_C = \frac{\sum_i g_i \, e^{-E_i/T} \sum_f C_{i,f}}{Z(H_2D^+)}, \tag{A.3}$$

where i and f refer to the rotational states of H_2D^+, and Z is the rotational partition function. The Oka & Epp coefficients $C_{i,f}$ are normalized so that k_C approaches in warm gas the Langevin rate coefficient for ion-molecule collisions.

We note that our definition of the collisional rate, $k_C n(H_2)$, includes collisions with both p-H_2 and o-H_2, and the rates of both o-p and p-o conversions of H_2D^+.

2) When collisions dominate, the relative populations within the ortho and para states approach those in thermal equilibrium, although o/p H_2D^+ can be non-thermal. This is equivalent to the assumption that the rotationally inelastic collisions, i.e., o-o and p-p transitions, are fast compared to nuclear spin changing reactions.

3) Reactions (A.1) and (A.2) describe nuclear spin-changing collisions summed up over all states, and determine o/p H_2D^+. The following conditions are obtained for the state-to-state coefficients $C_{pi,of}$ and $C_{oi,pf}$ corresponding to para-ortho and ortho-para transitions, respectively:

$$\frac{\sum_i g_{pi} \, e^{-E_{pi}/T} \sum_f C_{pi,of}}{Z(p-H_2D^+)} = o/p\,H_2\, k_1^+ + k_2^- \tag{A.4}$$

$$\frac{\sum_i g_{oi} \, e^{-E_{oi}/T} \sum_f C_{oi,pf}}{Z(o-H_2D^+)} = o/p\,H_2\, k_2^+ + k_1^-. \tag{A.5}$$

The partition functions $Z(p-H_2D^+)$ and $Z(o-H_2D^+)$ have a common zero-energy level (the ground state of para-H_2D^+). Equations (A.4) and (A.5) constrain the corresponding sums for the p-p and o-o coefficients, $C_{pi,pf}$ and $C_{oi,of}$, through assumption 1).

We assume that o/p H_2D^+ can be obtained from the condition of chemical equilibrium:

$$o/p\,H_2D^+ = \frac{o/p\,H_2\, k_1^+ + k_2^-}{o/p\,H_2\, k_2^+ + k_1^-}. \tag{A.6}$$

The coefficient k_2^- is very small at low temperatures, and Eq. (A.6) is essentially the same as Eq. (7) in Gerlich et al. (2002). By substitution one finds that a thermal o/p H_2 ($\sim 9 e^{-170.4\ K/T}$) makes also o/p H_2D^+ thermal ($\sim 9\, e^{-86.4\ K/T}$).

The collisional coefficients satisfy the principle of detailed balance, i.e., $n_i C_{if} = n_f C_{fi}$ when the relative populations are given by the Boltzmann distribution. The normalization described above ensures that this is also true for ortho-para transitions even if o/p H_2D^+ is non-thermal.

In practice, all state-to-state collisional rate coefficients were initially calculated using the Oka & Epp formula. The rate coefficients *between* the ortho and para states were then scaled using (A.4) and (A.5). Thereafter rate coefficients *within* ortho and para states were normalized so that assumption 1) is satisfied.

We used the following values for the total rate coefficients in reactions (A.1) and (A.2): $k_1^+ = 2 \times 10^{-9}$ $cm^3\,s^{-1}$, $k_1^- = k_1^+ e^{-84\ K/T}$, $k_2^+ = k_1^+/18$, and $k_2^- = k_2^+ e^{-257\ K/T}$ (Walmsley et al. 2004, the k_2 coefficients are slightly modified to account for the spin statistics). The o/p ratio was assumed to be 10^{-4}, which is believed to be characteristic of a dense dark cloud at an advanced chemical stage (Walmsley et al. 2004; Flower et al. 2006).

In very dense gas collisional transitions between the lowest rotational states of both para- and ortho-H_2D^+ can compete with radiative transitions. For example, the observed ground-state ortho line ($1_{10} \rightarrow 1_{11}$) is thermalized in the core centre (see Fig. 2, middle panel).

The collisional coefficients derived here have a steeper temperature dependence than those used by van der Tak et al. (2005) which are proportional to the square root of the kinetic temperature. The (downward) collisional coefficient for the $1_{10} \rightarrow 1_{11}$ transitions has, however, a relatively smooth slope between ~7 and ~9 K, where the average value is $\sim 2 \times 10^{-10}$ $cm^3\,s^{-1}$. This number corresponds to the best-fit value that van der Tak et al. (2005) obtained by scaling the Black et al. (1990) coefficient by a factor of ~5.

References

Alves, J. F., Lada, C. J., & Lada, E. A. 2002, Nature, 409, 159
Bacmann, A., André, P., Puget, J.-L., et al. 2000, A&A, 361, 555
Bacmann, A., Lefloch, B., Ceccarelli, C., et al. 2002, A&A, 389, L6
Bergin, E. A., & Tafalla, M. 2007, ARA&A, 45, 339
Bergin, E. A., Alves, J., Huard, T., & Lada, C. J. 2002, ApJ, 570, L101
Bergin, E. A., Maret, S., van der Tak, F. F. S., et al. 2006, ApJ, 645, 369
Black, J. H. 1994, in The First Symposium of the Infrared Cirrus and Diffuse Interstellar Clouds, ASP Conf. Ser., 58, 355
Black, J. H., van Dishoek, E. F., Willner, S. P., & Woods, R. C. 1990, ApJ, 358, 459
Burke, J. R., & Hollenbach, D. J. 1983, ApJ, 265, 223
Caselli, P., Walmsley, C. M., Tafalla, M., Dore, L., & Myers, P. C. 1999, ApJ, 523, L165
Caselli, P., van der Tak, F. F. S., Ceccarelli, C., & Bacmann, A. 2003, A&A, 403, L37
Crapsi, A., Caselli, P., Walmsley, C. M., et al. 2005, ApJ, 619, 379
Crapsi, A., Caselli, P., Walmsley, C. M., & Tafalla, M. 2007, A&A, 470, 221
Evans, N. J. II, Rawlings, J. M. C., Shirley, Y. L., & Mundy, L. G. 2001, ApJ, 557, 193
Flower, D. R., Pineau des Forêts, G., & Walmsley, C. M. 2006, A&A, 449, 621
Gerlich, D., Herbst, E., & Roueff, E. 2002, Planet. Space Sci., 50, 1275
Güsten, R., Nyman, L.-Å., Schilke, P., et al. 2006, A&A, 454, L13
Hugo, E., Asvany, O., Harju, J., & Schlemmer, S. 2007, in Molecules in Space and Laboratory, meeting held in Paris, France, May 14–18, ed. J. L. Lemaire, & F. Combes, 119
Juvela, M. 1997, A&A, 322, 943
Kirk, J. M., Ward-Thompson, D., & André, P. 2005, MNRAS, 360, 1506
Knude, J., & Høg, E. 1998, A&A, 338, 897
Miller, S., Tennyson, J., & Sutcliffe, B. T. 1989, Mol. Phys., 66, 429
Motte, F., André, P., & Neri, R. 1998, A&A, 336, 150
Oka, T., & Epp, E. 2004, ApJ, 613, 349
Ossenkopf, V. H., & Henning, T. 1994, A&A, 291, 943
Park, K., & Light, J. C. 2007, J. Chem. Phys., 126, 044305-1–19
Stamatellos, D., & Whitworth, A. P. 2003, A&A, 407, 941
Steinacker, J., Bacmann, A., Henning, Th., Klessen, R., & Stickel, M. 2005, A&A, 434, 167
Tafalla, M., Santiago-García, J., Myers, P. C., et al. 2006, A&A, 455, 577
van der Tak, F. F. S., Caselli, P., & Ceccarelli, C. 2005, A&A, 439, 195
Vastel, C., Phillips T. G., & Yoshida, H. 2004, ApJ, 606, L127
Walmsley, C. M., Flower, D. R., & Pineau des Forêts, G. 2004, A&A, 418, 1035
Willacy, K., Langer, W. D., & Velusamy, T. 1998, ApJ, 507, L171
Zucconi, A., Walmsley, C. M., & Galli, D. 2001, A&A, 376, 650